In situ monitored stretching induced α to β allotropic transformation of flexible poly(vinylidene fluoride)-CoFe2O4 hybrid films: The role of nanoparticles inclusion

Chirine Ben Osman, Sophie Nowak, Alexis Garcia-Sanchez, Yann Charles, Souad Ammar, Silvana Mercone, Fayna Mammeri

Accepted Manuscript

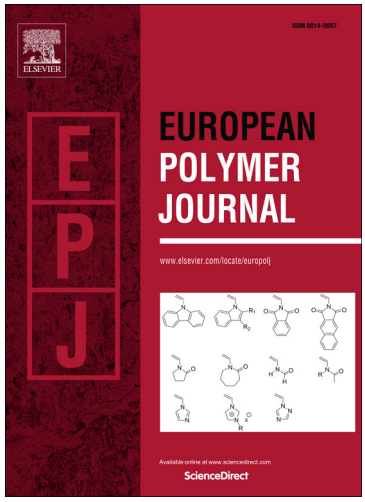

In situ monitored stretching induced α to β allotropic transformation of flexible poly(vinylidene fluoride)-$CoFe_2O_4$ hybrid films: the role of nanoparticles inclusion

Chirine Ben Osman, Sophie Nowak, Alexis Garcia-Sanchez, Yann Charles, Souad Ammar, Silvana Mercone, Fayna Mammeri

PII: S0014-3057(16)30594-8
DOI: http://dx.doi.org/10.1016/j.eurpolymj.2016.09.056
Reference: EPJ 7530

To appear in: *European Polymer Journal*

Received Date: 15 June 2016
Revised Date: 23 September 2016
Accepted Date: 28 September 2016

Please cite this article as: Ben Osman, C., Nowak, S., Garcia-Sanchez, A., Charles, Y., Ammar, S., Mercone, S., Mammeri, F., *In situ* monitored stretching induced α to β allotropic transformation of flexible poly(vinylidene fluoride)-$CoFe_2O_4$ hybrid films: the role of nanoparticles inclusion, *European Polymer Journal* (2016), doi: http://dx.doi.org/10.1016/j.eurpolymj.2016.09.056

In situ monitored stretching induced α to β allotropic transformation of flexible poly(vinylidene fluoride)-$CoFe_2O_4$ hybrid films: the role of nanoparticles inclusion

Chirine Ben Osman [a], Sophie Nowak [a], Alexis Garcia-Sanchez [b], Yann Charles [b], Souad Ammar [a], Silvana Mercone [b,*], Fayna Mammeri [a,*]

[a] *ITODYS, Université Paris Diderot, Sorbonne Paris Cité, CNRS UMR-7086, Paris, France.*

[b] *LSPM, Université Paris Nord, Sorbonne Paris Cité, CNRS UPR-3407, Villetaneuse, France.*

** E-mail: fayna.mammeri@univ-paris-diderot.fr; silvana.mercone@univ-paris13.fr*

Keywords

PVDF; magnetoelectric; near-field microscopy; phase transformation; fibrillary crystals; magnetic nanoparticle.

Abstract

The purpose of this work is to promote and optimize the formation of the β poly(vinylidene fluoride) (PVDF) phase, known to exhibit the maximum piezoelectric and ferroelectric properties, in free PVDF film as well as in hybrid one containing ferrimagnetic cobalt ferrite nanoparticles inclusions ($CoFe_2O_4$ NPs). In practice, uniaxial stretching was applied on both α-neat PVDF and α/β PVDF hybrid films, and the α to β transformation was followed by *in situ* near-field AFM observations and *ex situ* XRD, FTIR and DSC experiments. A strong influence of the nano-inclusions was observed on the mechanically induced allotropic transformation. They clearly promote the growth of the electroactive β phase in the PVDF matrix and favour the improvement of the whole film crystallinity. The proposed flexible material processing is easy-to-achieve and low cost. It is very promising for architecting original and smart magnetoelectric devices, in which the piezoelectric phases (β-PVDF) could be well interfaced with the magnetostrictive ones ($CoFe_2O_4$).

Introduction

Poly(vinylidene fluoride) (PVDF) and its copolymers [1] are widely used as polymeric ferroelectric material in the field of micro-electronic devices, high-charge storage [2] and energy conversion [3] thanks to their excellent piezoelectric/ferroelectric properties [4-6], dielectric feature and elasticity and flexibility [7]. Focusing on PVDF, it is well established that its final crystalline structure strongly affects its ferroelectric behavior [8]. Depending on its processing conditions, it can crystallize in various allotropic forms [4] known as non-polar α and ε phases and polar β, γ and δ phases. The α and β are the most commonly obtained. The α phase (trans-gauche bond conformation TGTG') is formed by cooling from the melt or by solvent cast at a temperature above 120°C [9-11], whereas the β one (all trans planar zigzag conformation TTTT) is obtained by solution casting from polar solvents under controlled operating conditions [12]. Typically, the annealing temperature must not exceed 70°C to avoid the simultaneous formation of α phase [6]. Unfortunately, low processing temperatures (T < 70 °C) lead to the production of highly porous, opaque, brittle and consequently hardly polarizable films. Since the β phase is much tricky and most technologically desirable [13-15], many material processing investigations were carried out in order to preferentially elaborate β-PVDF films exhibiting the best mechanical [16] and electrical properties. For such a purpose, the application of a high uniaxial pressure (15 MPa) on films processed at 140 °C was successfully achieved [10,17]. Interestingly, the resulting films appeared to be non-porous, transparent, flexible and highly polarizable. Uniaxial mechanical loading was also tested on α-PVDF films [18-20] to induce the reorientation of the polymer chains according to the β-trans-planar zigzag (TTT) conformation. In this latter case, all dipoles arranged perpendicularly to the direction of the applied stress. Several works were then reported dealing with the influence of tensile conditions over the mechanically induced α to β transformation. The impact of the operating temperature and the reached elongation $R = \Delta L_{final}/L_0$

on the content and the orientation of β phase were particularly investigated: β films can be obtained by working between 70 °C and 100 °C and limiting R within the 3 to 5 range [10,19,21-24]. Beside, the high mobility of macromolecular chains at high temperature makes the highest stretching temperatures (above 120 °C) less desirable since they reduce the phase transition efficiency. A compromise was found by fixing R to its highest value, *i.e.* 5 [19]. The improvement of the α to β transformation was also achieved by applying a poling. Samples presenting the highest content of β phase (T = 80 °C and R = 5) were the ones poled by the corona charge method using a suitable electric field. The orientation of the dipoles along the electric field direction was thus favored leading to a better intrinsic polarization in the poled films compared to the simple stretched ones [25]. It is important to note that in all these works, based on a uniaxial tension process [19,22,28-30], only few of them were interested by *in situ* measurements and observations. To the best of our knowledge, Li *et al.* [31] and Guo *et al.* [32] performed such an investigation using tensile stress tester under polarizing microscope. Also, Wu *et al.* [33] used the same kind of tester for *in situ* synchrotron wide angle X-ray diffraction (WAXD) and Small Angle X-ray scattering (SAXS) experiments to investigate the internal fiber morphology in PVDF films during deformation.

The effect of a biaxial tension process on the content and orientation/alignment of β crystallites was also explored [26]. FTIR spectroscopy combined to WAXD analysis at different elongation and deformation rate evidenced that these two processing parameters were very important for the desired allotropic transformation [26]. SAXS and WAXD measurements [27] revealed also morphological changes in the deformed zone near crack tips in α-PVDF films, highlighting the α to β transition.

It is worth noting that an alternative approach to increase the β phase ratio consists in adding inorganic nano-fillers to the PVDF matrix. There are an impressive number of studies in literature reporting the optimization of the electroactive β phase content by this route. Indeed, the flexibility of the polymer is expected to promote the strain transmission at the hybrid interface [34], allowing a better crystallization control of the β-PVDF phase, the nano-fillers acting as nucleating agents.

$BaTiO_3$ [35,36], Carbon Nanotubes (CNTs) [37], clays [37,38,39] and ferrite oxide nanoparticles (NPs) [40-42] were already used as nano-inclusions. Unfortunately, only few reports [43-44] mentioned the role played by the nano-fillers (shape, size, content) on the crystallization of the β-PVDF phase. Most of them [45,46] focused on the preparation and characterization of composite films obtained by simple dispersion of NPs (mainly iron oxides) in the preformed polymer. Some others described that the incorporation of NPs (typically cobalt ferrites) [46] led to high percentages of polar β phase in self-standing hybrid films processed at 80 - 100 °C.

Surprisingly enough, nothing is really stated in the literature on the combination of mechanical stretching and NPs incorporation. So far, there is no complete *in situ* nor *ex situ* study demonstrating clearly the process of the α to β transitions in PVDF-NP composite films under traction. To overcome this lack, we investigated the transition in uniaxially elongated α-neat and α/β-hybrid films. The hybrids consisted of 13 nm sized almost spherical polyol-made $CoFe_2O_4$ particles [46] dispersed in PVDF. *In situ* analyses were performed by coupling a tensile test machine to a near-field microscope (AFM) and *ex situ* ones were conducted on pre- and post-stretched films by X-Ray Diffraction (XRD), Infrared spectroscopy (IR) and Differential

Scanning Calorimetry (DSC). At the end, dynamic mechanical analysis (DMA) was performed and the obtained results were correlated to the mechanical properties of the films.

Experimental

A Nanoparticles synthesis

13 nm $CoFe_2O_4$ NPs were elaborated by the well-known polyol process, consisting in the forced hydrolysis of anhydrous $Fe(CH_3COO)_2$ (Sigma-Aldrich, 95%) and $Co(CH_3COO)_2,4H_2O$ (Sigma-Aldrich, 99%) in a polyol, namely triethyleneglycol (ACROS Organics, 98%). Thanks to its high relative permittivity and high boiling temperature (280 °C), the polyol acts as a solvent for the precursor salts and allows carrying out hydrolysis and condensation reactions under atmospheric pressure in a large temperature range. As previously described [46], the chemical composition, structure, size and size distribution of the produced NPs were checked by combining X-ray Fluorescence spectroscopy, X-ray diffraction and TEM observation.

B Film preparation

100 mg of PVDF powder (Aldrich, M_w = 534 000 g mol^{-1}) was dissolved in 1 mL of anhydrous N,N dimethylformamide, abbreviated as DMF (Sigma-Aldrich, 99.8%) under mechanical and then ultrasonic stirring at 25 °C. The resulting solution was deposited to form a continuous polymer film using the doctor blade technique. In practice a casting knife from Elcometer was employed to control the final film thickness in the 20 - 70 µm range. PVDF–$CoFe_2O_4$ hybrid films were prepared in a similar way. 1 mg of $CoFe_2O_4$ NPs was dispersed in a solution of 100 mg of PVDF in 1 mL of DMF (1 wt.-%). Neat PVDF films were thermally treated in an oven at 240 °C for 30 min leading predominantly to α-PVDF while hybrid films were melt processed at 80 °C during 1 hr. The films, of 1 × 10 cm^2 lateral size, were finally peeled off from glass substrates by diving them into cold water.

C Tensile test coupled to *in situ* Near-Field Microscopy and *ex situ* X-ray Diffraction

A micro-tensile 300 N Deben™ tester, able to apply loads up to 300 N, was used. It was equipped with a 75 N load cell enabling the force measurement with an accuracy of 0.1 N. It was employed within the uniaxial stretching configuration, fixing the stretching rate to 0.1 mm min^{-1}. It was also coupled to an AFM to study the film morphology. The sample surface was imaged at room temperature in the standard tapping mode of a Scan Probe Microscopy apparatus by VEECO (DI-3100 Model) Silicon Tips with a K = 40 N W^{-1} and resonance frequency ν = 300 kHz. Height images were collected for each sample and analyzed using the NANOSCOPE Analysis program.

The crystalline quality of the prepared films was checked by XRD. Typically, their θ-θ patterns (2θ = 15-40°, 0.025°) were recorded before and after stretching using an Empyrean (PANALYTICAL) diffractometer equipped with a multichannel PIXcel 3D detector, 0.04 rad Soller slits and a Cu Kα X-ray source (1.5418 Å, 45 kV and 40 mA). Structure analysis was performed using HIGHSCORE software (diffraction peaks of α and β phases were identified according to ICCD files n°00-042-1650 and n°00-042-1649, respectively).

D *Ex situ* Infrared spectroscopy and Differential Scanning Calorimetry

All the infrared spectra were recorded (ν = 4000-650 cm^{-1}, 4 cm^{-1}) on a ThermoNicolet 8700 spectrophotometer using an ATR instrument to quantify the β phase content before and after uniaxial tension process. Finally, DSC was performed with a TA Q20 equipment under N_2 atmosphere at a heating rate of 10 °C min^{-1} to evaluate the crystalline fraction of the polymer before and after stretching.

E Dynamic Mechanical Analysis

In order to study the viscoelastic properties of PVDF, DMA was performed using Electroforce 3100. A sinusoidal strain was applied at room temperature by varying the frequencies from 1 to

10 Hz, at a speed of 0.2 mm s^{-1} and with an amplitude not exceeding 10 %. In all the cases, a small pre-tensile load was applied to properly position the sample between the jaws. At the end, the collected strain vs. deformation data allowed the determination of the complex modulus.

Results and discussion

A Stretching induced α to β transformation in neat PVDF films

During stretching a film whitening was observed, marking the phase transformation beginning. According to previous studies [21-23], the mechanical deformation is expected to improve the development of the β phase through a stress induced crystallization process.

Near-field microscopy imaging of the surface morphology during the uniaxial tension process evidenced also significant changes. These changes are well-illustrated by the optical images captured for each stretched sample state (Figure 1a,b,c), before engaging the AFM tip: an evolution from a spherulitic structure to a fibrillar one is unambiguously observed. So in the 6% elongated film well-defined large spherulites, assigned to the non-electroactive α phase [47-49], are present (Figure 1a), while in the 28% elongated one (Figure 1b), the spherulites are destabilized and start to align along the uniaxial traction direction giving rise to the fibrillar morphology. Darker transversal "belts" between the reorganized spherulite zones also appear (Figure 1g). This phenomenon is accompanied by the emerging of fibrillar new presumably crystalline structures in the AFM Ƶ-images (Figure 1e,f). While the deformation increases, transversal belts narrow and the amount of the fiber phase increases and becomes predominant in the observed areas (Figure 1c,g). At the end, almost 80% of the imaged surface is transformed from the spherulite morphology (Figure 1a,b) to the fibrillar one (Figure 1c,g). Attributing the latest morphology to the β phase structure [43-45], one can assume that by this process, 80 % of the film has gone under α to β transformation.

These observations suggest that the formation of β phase starts from the middle of the stretched sample and progressively extends to its border, in good agreement with previous results [31].

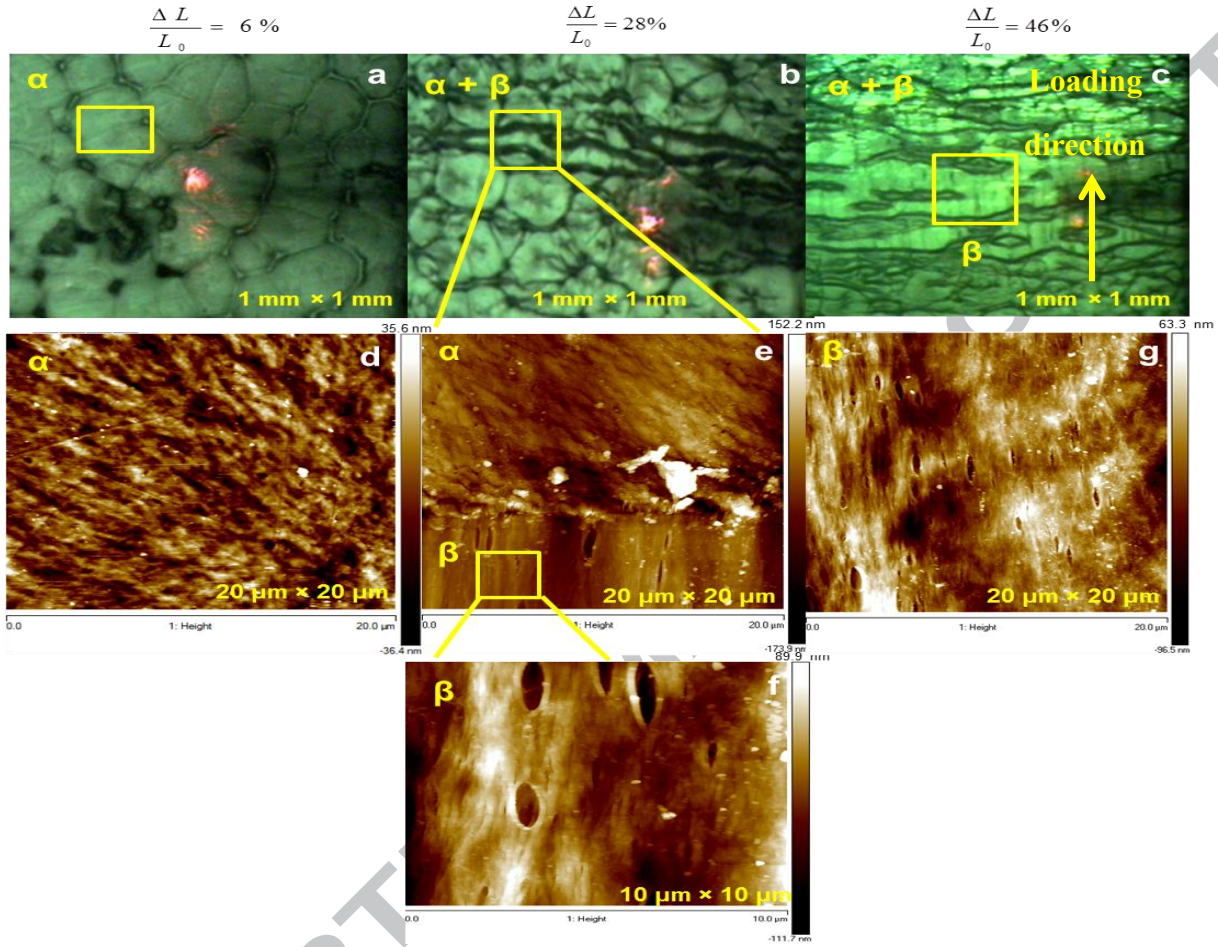

Figure 1. Optical microscopy (a, b, c) and AFM pictures (d, e, f, g) for different stretched states. Granular morphology (α phase) is clearly observed in d and e while fibrillar morphology (β phase) is revealed in f and g. $\Delta L_{final}/L_0$ refers to the maximal strain applied to the deformed sample.

On the film elongated at 40% and assumed to be rich in β phase, AFM Ƶ- images were collected at different scales. Focusing on the 25 µm × 25 µm images, one can easily observe aligned fibers of 0.7 to 1.3 µm in width (Figure 2). Moreover, the fibers appear to be composed

of transversal lamellae. Unfortunately, we could not go further than an elongation of 46% (*i.e.* 80% of transformation) of the film putting in evidence its mechanical fragility, most probably due to its high crystallinity degree. According to literature, the *β* phase can be transformed by mechanical deformation from *α* phase through a transformation efficiency linearly proportional to the stress value. The mechanical properties of the film did not allow a 100% transformation.

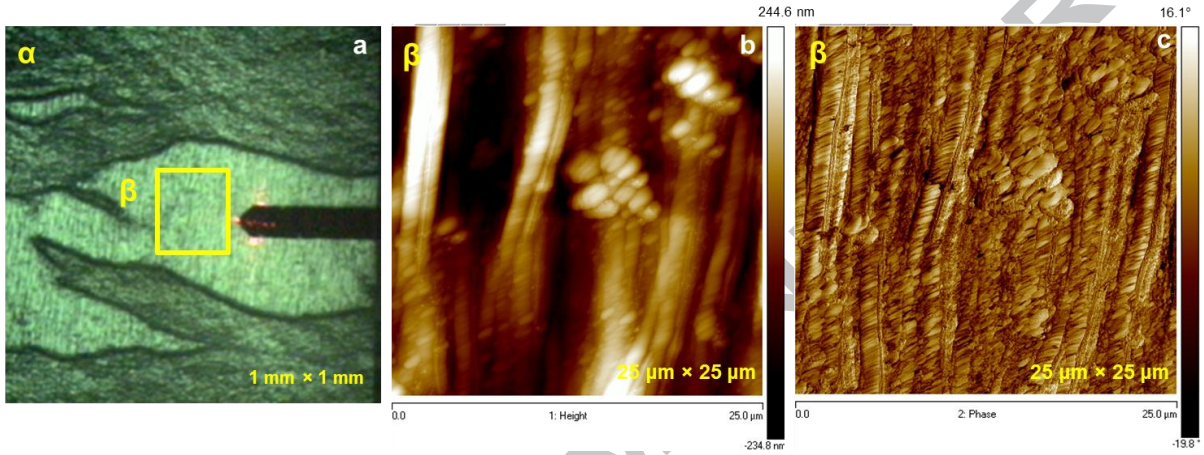

Figure 2. Optical microscopy (a) and AFM images (b, c) of neat PVDF film elongated at 40%; the fibrillar morphology (β-phase) is analyzed both by Ƶ-image (b) and deflection one (c).

To complete this study, the IR spectra of neat PVDF films were collected before and after uniaxial tensile process (Figure 3) and compared (see experimental section). The respective amounts of apolar *α* and polar *β* phases were determined through the analysis of the specific absorption bands of each phase [2,50]. IR spectra were normalized to be comparable by using the 875 cm^{-1} band (showing a stable intensity). Two different absorption bands at 762 cm^{-1} and 840 cm^{-1} are in fact characteristics of *α* and *β* phases respectively. Assuming that the infrared absorption follows the Beer-Lambert law, the A_α and A_β absorbances, at 762 cm^{-1} and 840 cm^{-1} respectively, are given by Eq. 1:

$$A_{\alpha,\beta} = Log\left(\frac{I^0_{\alpha,\beta}}{I_{\alpha,\beta}}\right) = C \times K_{\alpha,\beta} \times X_{\alpha,\beta} \times L \qquad \text{Eq. 1}$$

Where L is the sample thickness, C is the average monomer concentration, α and β refer to the allotropic phases, I_0 and I are the incident and transmitted intensities of the radiation, K is the absorption coefficient at the respective wavenumber, and X is the degree of crystallinity of each phase. The value of K_α is 6.1×10^4 cm^2 mol^{-1} and K_β is 7.7×10^4 cm^2 mol^{-1} [51]. For a system containing α and β phases, the relative fraction of the β phase, F(β), can be calculated using Eq. 2:

$$F(\beta) = \frac{X_\beta}{X_\alpha + X_\beta} = \frac{A_\beta}{\left(\frac{K_\beta}{K_\alpha}\right) \times A_\alpha + A_\beta} = \frac{A_\beta}{1.26A_\alpha + A_\beta} \qquad \text{Eq. 2}$$

In the present case, the intensity of the characteristic α phase bands (762, 796, 976, 1210, 1383 cm^{-1}) decreases, but does not disappear, after stretching, while that of the β phase bands (840 and 1275 cm^{-1}) increases. It should be noted that mostly all the absorption bands of β and γ phases are overlapped. However, we can distinguish between the two phases by the band centered at 1234 cm^{-1}, which is unique for the γ phase. The distinction between these two piezoelectric phases is extremely important, since the β one is the most desirable form [52-53]. The intensity of this band in the recorded spectra is relatively weak and almost constant (see Figure 3), making our quantification of the relative fraction of the β phase, F(β), quite significant for the studied samples. Values of 25 and 48% were thus obtained on elongated films at 6% and 46%, respectively. These results support also the uncompleted transformation observed by AFM.

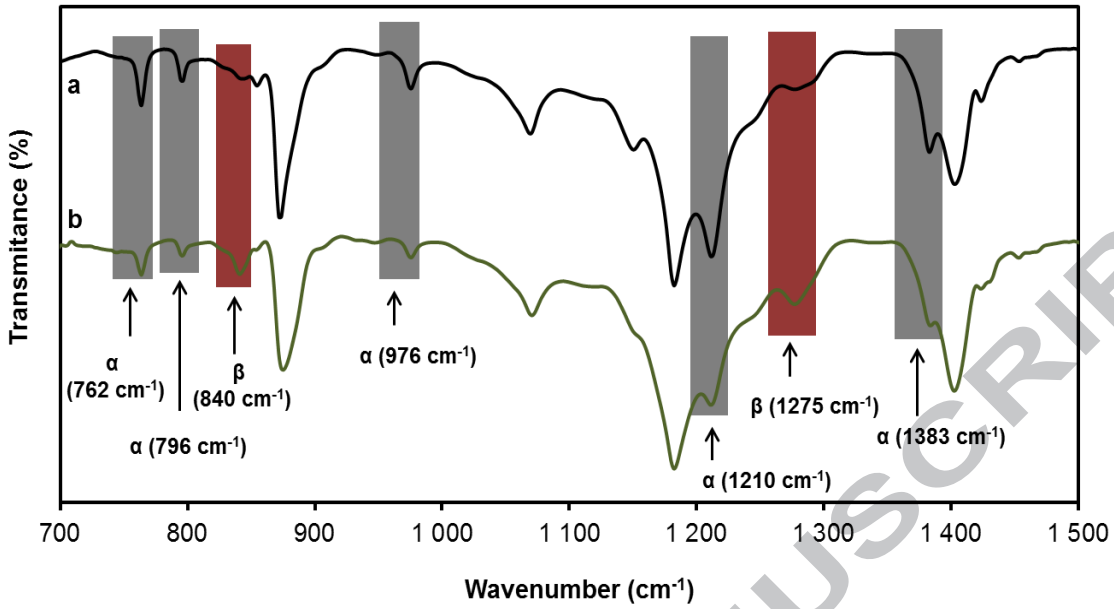

Figure 3. IR spectra of neat PVDF film before (a) and after (b) mechanical loading.

The degree of crystallinity of PVDF (including polar and apolar polymorphs) was deduced from differential scanning calorimetry (DSC) experiments (see Supporting File, Figure S1) using Eq. 3:

$$X_c^{c/m} = \frac{\Delta H_{c/m} \times 100}{x \times (\Delta H_{100\%\ crystalline})_\alpha + y \times (\Delta H_{100\%\ crystalline})_\beta} \qquad \text{Eq. 3}$$

where x and y are the weight fraction of the α and β phases, respectively, $(\Delta H_{100\%\ crystalline})_\alpha$ and $(\Delta H_{100\%\ crystalline})_\beta$ are the enthalpy of pure crystalline α- and β-PVDF phases, equal to 93.04 and 103.4 J g^{-1}, respectively [4]. The recorded DSC thermograms revealed that the degree of crystallinity of uniaxially oriented PVDF, sharply increased from 36.3 to 87.0% indicating that the strain promotes the crystallization of β phase from the α one and induces an improvement of the whole film crystallinity.

The α to β transformation was investigated also by *ex situ* X-ray diffraction. The pattern of neat PVDF (Figure 4) displays four intense peaks at 2θ = 17.8°, 18.3°, 19.9°, and 26.6° [43,54,55]

associated to (100), (020), (110) and (021) reflections of the monoclinic α phase. The pattern of the elongated film at 46% displays almost the same peaks, their 2θ positions being slightly shifted to higher values for some of them. Typically, the peak at 19.9° is shifted to 20.10° [43,54,55] and assigned to (110) and (200) reflections of the orthorhombic β phase. The peak at 18.3° is shifted to 18.5° and assigned to the overlapping of the α and γ (020) lines. Note that the intensity of α phase diffraction peak at 26.6° decreases significantly after stretching, confirming the α to β transformation, in agreement with AFM and IR investigations.

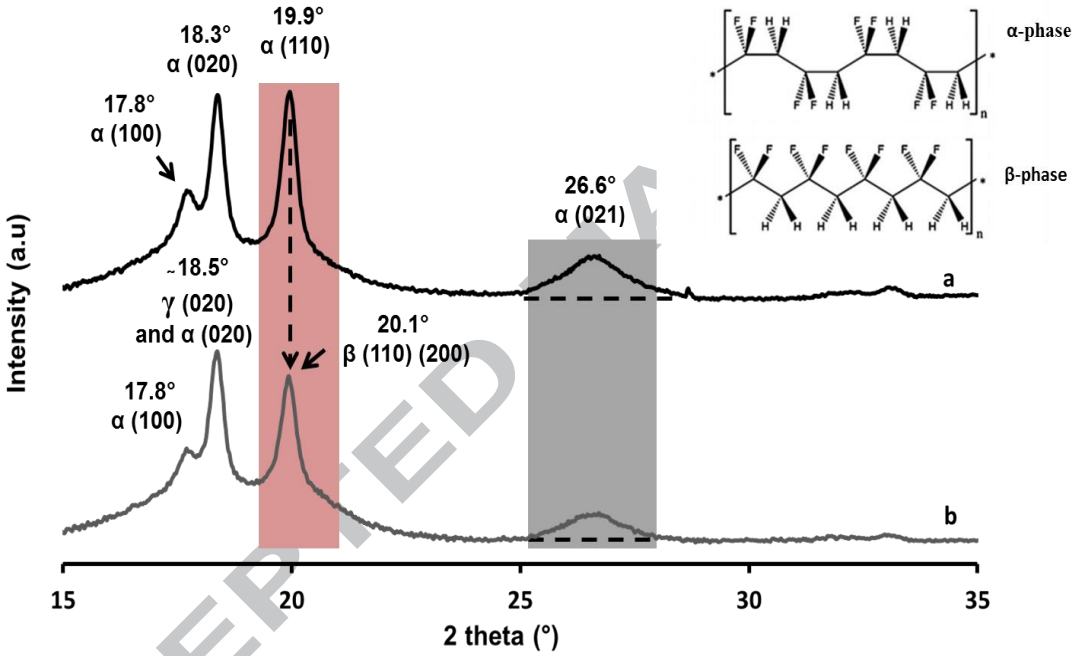

Figure 4. XRD patterns of neat PVDF films obtained before (a) and after (b) uniaxial tension loading.

B Stretching induced α-to-β phase transformation in hybrid PVDF films

After the introduction of 1 wt.-% of 13 nm sized $CoFe_2O_4$ NPs inside the PVDF matrix [46], and before any mechanical treatment, the nominal F(β) content of the electroactive β phase is found to be about 68% (determined by Eq. 2). This relatively high percentage of the β phase is confirmed

by AFM observations (Figure 5e). Clearly, spherulite (α) and fibrillar (β) morphologies co-exist. By stretching, the β content increases: an elongation of 13.5% induces a film whitening, marking again the beginning of the α to β transition, and transversal belts appear (Figure 5b,c,d). An elongation of 47%, induces the predominance of the oriented β phase (Figure 6a). Micrometric spherulites constituted of nanofibers appear (Figure 6b), suggesting that the reorientation of the polymer chains starts first inside the spherulites.

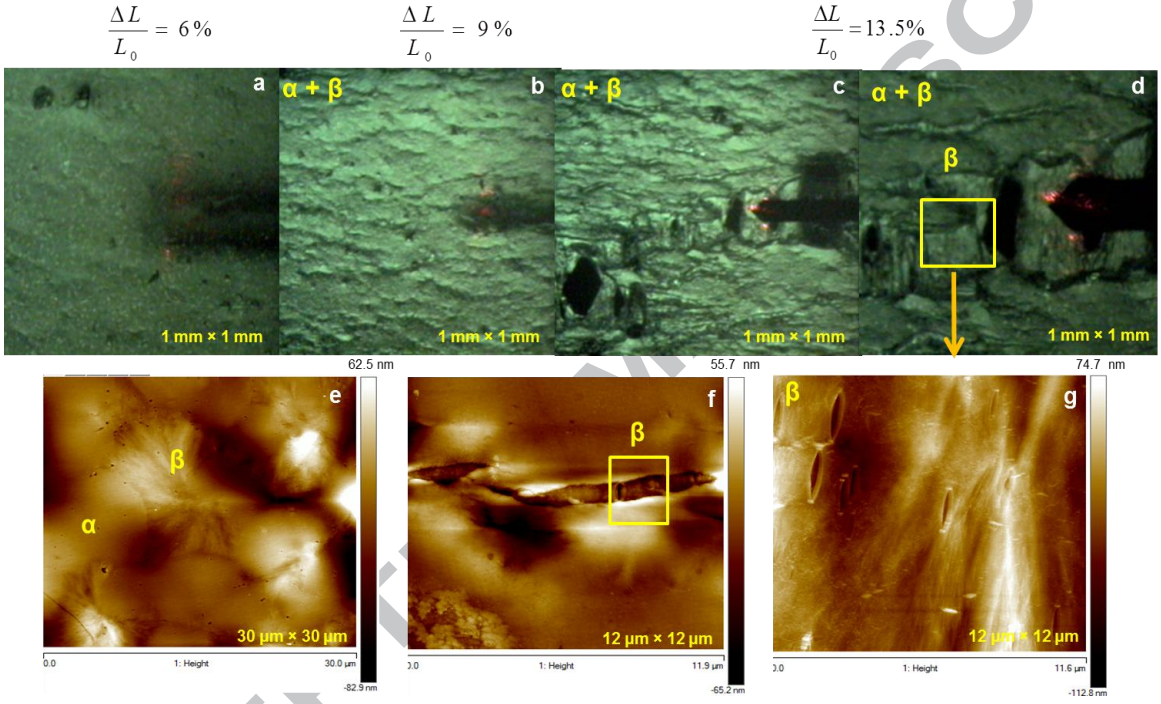

Figure 5. Optical microscopy (a, b ,c, d) andAFM (e, f, g) images of the hybrid PVDF film containing 1 wt.% $CoFe_2O_4$ NPs under mechanical loading. Mixed area (α+β phases) is visible in (e) while the fibrillar morphology (β phase) is easily observable in (f, g).

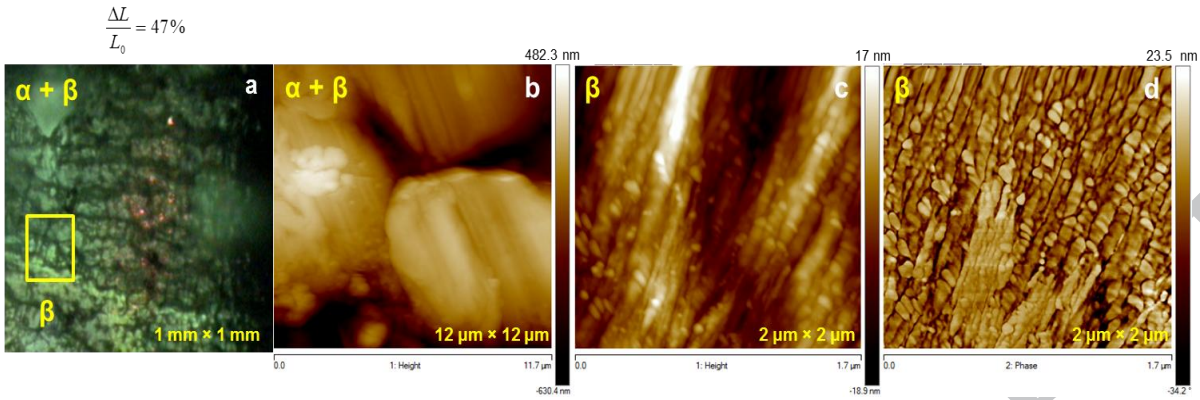

Figure 6. Optical microscopy (a) and AFM (b, c, d) images of the hybrid PVDF film containing 1 wt.-% $CoFe_2O_4$ NPs stretched to a final elongation of 47%; (b), zoom-in of the yellow square; fibrillar morphology (c, d) characteristic of β phase; Ƶ (c) and deflection (d) images.

The width of the fibers was estimated (Figure 6c,d). It varies from 40 to 100 nm, one order smaller than that measured on stretched neat PVDF films, traducing a confinement effect of the fibrillary morphology inside the micrometric spherulites. All these features clearly evidence that the presence of NPs strongly influences the process of the α to β transformation. The polymer chains reorientation still starts inside the spherulite during stretching. It propagates afterwards from one spherulite to another, but it is reasonable to figure out that this propagation is not fully allowed by the presence of the nano-inclusions. This explains why the β fibers are so thinner in the hybrid film compared to the neat one.

It is worth noted that in spite of these differences, the granular structures of the fiber are still present, as observed in the neat PVDF film. The structure evolution of the composite films was also investigated by IR spectroscopy and the relative β phase fraction was quantified and compared before and after stretching, using Eq. 2. The infrared spectrum of the film after an elongation of 47% (Figure 7b) demonstrates that the bands at 762, 796, 976, 1210 and 1383 cm^{-1}, characteristic of α phase, disappeared and/or reduced while the characteristic band of β phase at

840 and 1275 cm^{-1} increased confirming the phase transformation. The F(β) was found to increase from 68% to 79% upon increasing the deformation from 0 to 47%, confirming the AFM results.

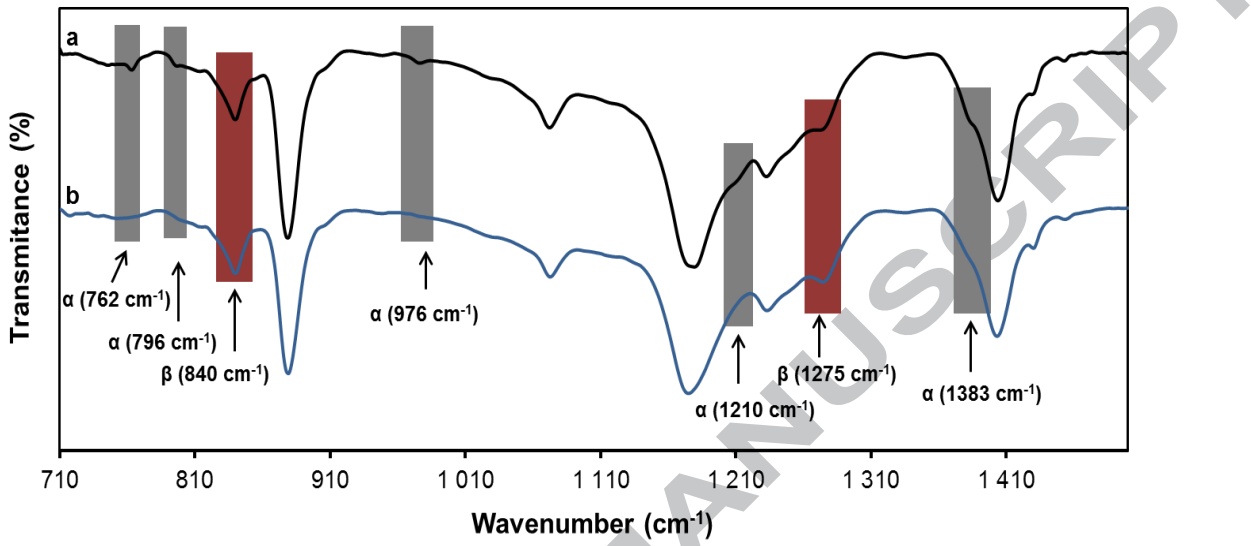

Figure 7. IR spectra of hybrid PVDF film (1 wt.-% $CoFe_2O_4$) before (a) and after (b) uniaxial loading.

The XRD patterns of the as-produced hybrid film (Figure 8) revealed a strong diffraction peak at 20.3° which means that the β phase is the predominant crystalline PVDF phase. A large shoulder at lower diffraction angles, around 19°, ascribed to the presence of α and γ phases [55] or to a distorted β one [60] was also evidenced.

Elongated to 47%, a weaker shoulder was detected and the reflection peak of the β phase becomes tighter which could indicate the transformation of the distorted β or γ conformations to a more crystalline β phase. The appearance of a small peak at 36.2° [61] assigned to the reflections (020) and (101) of β phase highlights the efficiency of this phase transformation. Note that the peak at 28.5° could be assigned to the (211) diffraction line of a metastable γ phase.

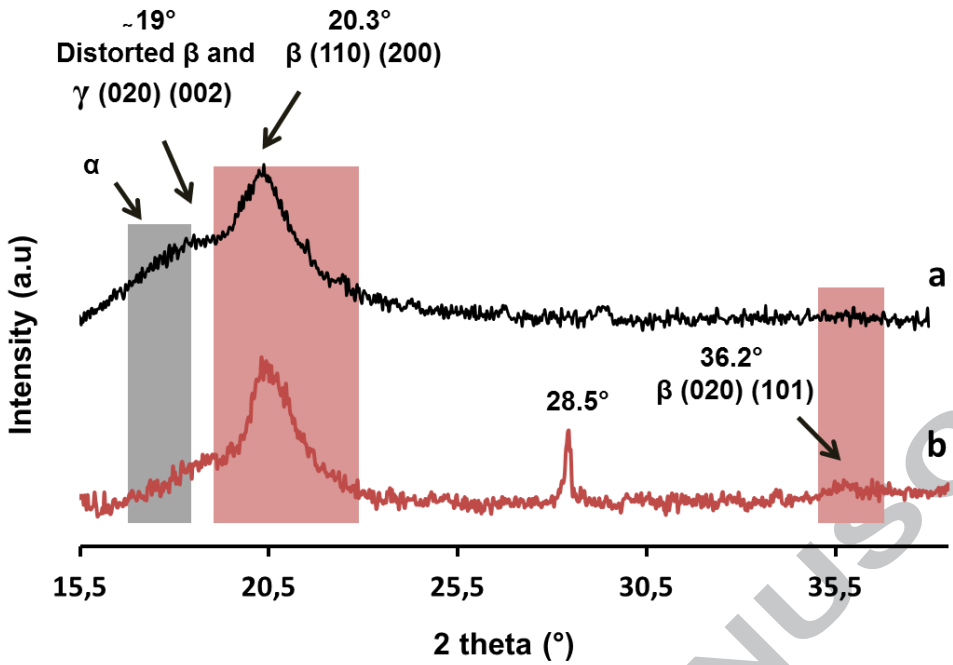

Figure 8. XRD patterns of hybrid film (1 wt.-% $CoFe_2O_4$) before (a) and after (b) uniaxial tension loading.

Beside, DSC measurements demonstrate an increase of the degree of crystallinity in the composite film upon mechanical stretching at a final elongation of 47%: X_m^c increases from 39.2 to 47.5% (see Supporting file, Figure S2). Hence, the phase transformation induces an improvement of the polymer crystallinity also in the presence of NPs. It is worth noted that the improvement in this case is less impressive than the one observed in the case of the neat PVDF film albeit their final β phase content is almost similar.

As reported in literature [56,57], it is now known that the nucleation of the electroactive β phase of the polymer is influenced by the interactions between ferrite NPs and PVDF. The strong interaction between the magnetic NPs (characterized by a negative zeta potential) and the CH_2 groups (exhibiting a positive charge density) tends to align the polymer chains at the surface of these NPs in an extended TTTT conformation favoring the crystallization of the β phase. It is also

interesting to notice that in previous works the inclusion of 30 to 50 nm NPs led to a decrease of the polymer crystallinity [58,59] suggesting that an important fraction of polymer chains was confined in interphases with the filler particle. In the present case, the mechanical deformation not only helps improving the content of β phase but also the crystallinity of both neat and hybrid films. This can be explained by the smaller size of the incorporated ferrite NPs than that of the previously used NPs in the literature. In other words, our inclusions seem to be less disturbing the polymer chain motions. Hence we can conclude that the presence of small NPs (typically 13 nm) rather than bigger ones (30 to 50 nm) promotes the crystallinity of PVDF based films as well as a higher content of polar phase during the mechanical deformation of the films.

In situ AFM imaging was performed on films containing 5 wt.-% of NPs but unfortunately they broke at small elongation values (i.e.< 16%) probably due to the toughness of the film caused by the presence of higher amounts of NPs and a quite high PVDF crystallinity ratio.

To deeply investigate the relationships between the introduction of NPs and the mechanical behavior of the resulting hybrid film, DMA experiments were performed on neat PVDF and PVDF containing 1 wt.-% of $CoFe_2O_4$ NPs. The evolution of the Young complex modulus |E*| with increasing frequencies is shown in Figure 9 for both samples. As expected, the value of |E*| is higher while dispersing 1 wt.-% of NPs in the PVDF matrix. |E*| increases with frequency in this latter case from 269 to 362 MPa compared to neat PVDF that highlights an increase from 89 to 218 MPa. This observation suggests that the presence of a small amount of NPs (1 wt.-%) increases the complex modulus of the composite leading to a higher stiffness of the material compared to the pure one. However, this reinforcement of the matrix does not seem to affect the deformation of the film neither its flexibility as confirmed by the elongation obtained during the *in situ* AFM observations (a deformation of 47% was achieved before film breaking).

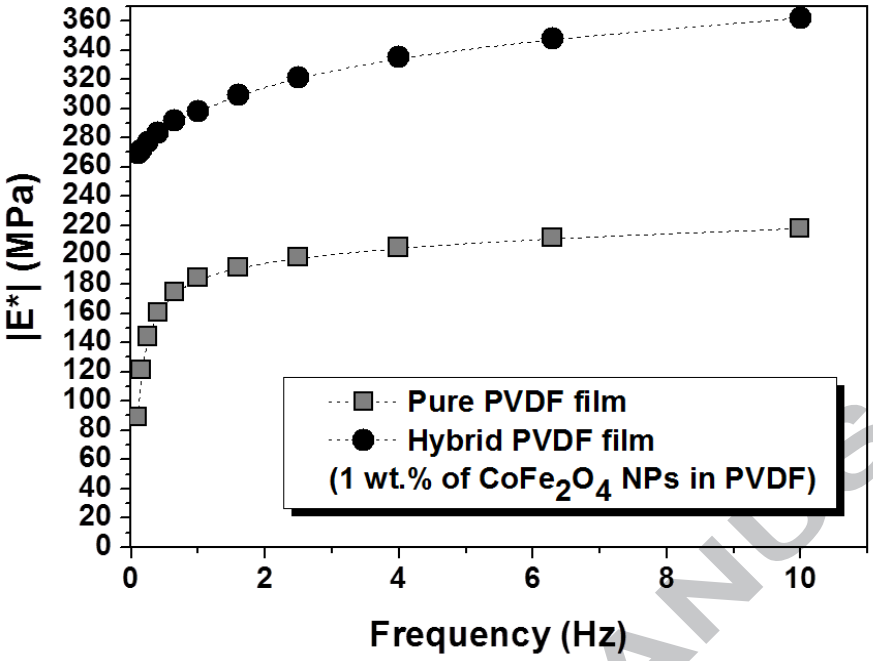

Figure 9. Modulus-frequency curves measured by DMA on neat PVDF (a) and PVDF containing 1 wt.-% $CoFe_2O_4$ NPs (b).

Conclusions

In conclusion, the process of strain-induced α to β transformation was monitored in α-neat and α/β-hybrid films by *in situ* coupling tensile test to near-field AFM. The phase transition was first observed by optical microscopy through the presence of transversal belts in the middle of the deformed spherulites. The AFM images, also consistent with the *ex situ* XRD experiments, highlighted that this phenomenon is accompanied by the appearance of a new fibrillary crystalline morphology, characteristic of the β phase. In uniaxially oriented hybrid films, the presence of the NPs impacts the transition mechanism from the one observed for the neat PVDF film since it affects the polymer chain reorientation. A confinement is observed which reduces the mean width of the formed fibers during the allotropic transformation. Indeed, while in the α-

neat film, the fibers are micrometric, they are submicrometric in the hybrid one. *Ex situ* IR and DSC analyses highlighted the improvement of the β phase content as well as the increase of the relative crystallinity of PVDF in stretched hybrid films. Stretching appears as a powerful technique to produce highly polarizable PVDF films whose polarizability can still be improved by introducing very low amounts of $CoFe_2O_4$ NPs compared to literature [62, 63]. The design of such flexible magneto-electric materials (exhibiting both piezoelectric and magnetic properties) can open the way for the development of a new generation of magnetic recording media, sensors and/or transducers. Magneto-electric measurements of our systems are in progress**.**

Author Information

Corresponding authors:

* E-mail: fayna.mammeri@univ-paris-diderot.fr and silvana.mercone@univ-paris13.fr

Acknowledgements

The authors are grateful to Alexandre Chevillot (Paris Diderot University), Damien Faurie and Isabelle Bataille (Paris Nord University), for their technical assistance in FTIR, *in situ* tensile tests and DMA, respectively. ANR (Agence Nationale de la Recherche) and CGI (Commissariat à l'Investissement d'Avenir) are gratefully acknowledged for their financial support of this work through Labex SEAM (Science and Engineering for Advanced Materials and devices), ANR 11 LABX 086, ANR 11 IDEX 05 02 and through the funding of MULTIFERROFLEX project (ANR-14-CE08-0005-01).

Notes and references

[1] Ameduri, B. From Vinylidene Fluoride (VDF) to the Applications of VDF-Containing Polymers and Copolymers: Recent Developments and Future Trends. *Chem. Rev*. **2009**, 109, 6632-6686.

[2] Lanceros-Mendez, S.; Mano, J. F.; Costa, A. M.; Schimdt, V. H. FTIR and DSC studies of mechanically deformed β-PVDF films. J. *Macromol. Sci. Phys.* **2007**, 40, 517-527.

[3] Qi, L.; Wang, Q. Ferroelectric Polymers and Their Energy-Related Applications. *Macromol. Chem. Phys*. **2016**, 217, 1228-1244.

[4] Lovinger, A. J. Annealing of Poly(viny1idene fluoride) and Formation of a Fifth Phase. *Macromolecules* **1982**, 15, 40-44.

[5] Nalwa, H. S. Ferroelectric Polymers, Marcel Dekker, New York, **1995.**

[6] Bauer, S. Poled polymers for sensors and photonic applications. *J. Appl. Phys.* **1996**, 80, 5531-5558.

[7] Martins, P.; Lanceros-Méndez, S. Polymer-Based Magnetoelectric Materials. *Adv. Funct. Mater.* **2013**, 23, 3371–3385.

[8] Yang. L.; Li. X.; Allahyarov. E.; Taylor. P.L.; Zhang. Q.M.; Zhu.L. Novel polymer ferroelectric behavior via crystal isomorphism and the nanoconfinement effect. *Polymer* **2013**, 54, 1709-1728.

[9] Gregorio, J. R.; Cestari, M. Effect of Crystallization Temperature on the Crystalline Phase Content and Morphology of Poly (vinylidene Fluoride). *J. Polym. Sci. Part B: Polym. Phys.* **1994**, 32, 859-870.

[10] Sencadas, V.; Filho, R. G.; Lanceros-Mendez, S. Processing and characterization of a novel nonporous poly(vinylidene fluoride) films in the β phase. *J. Non-Cryst. Solids* **2006**, 352, 2226–2229.

[11] Martins, P.; Nunes, J. S.; Hungerfordb, G.; Miranda, D.; Ferreira, A.; Sencadas, V.; Lanceros-Méndez, S. *Phys. Lett. A* **2009**, 373, 177-180.

[12] Benz, M.; Euler, W. B.; Gregory, O.J. The Role of Solution Phase Water on the Deposition of Thin Films of Poly (vinylidene fluoride). *Macromolecules* **2002**, 35, 2682-2688.

[13] Scott, J. F.; Applications of magnetoelectrics. *J. Mater. Chem*. **2012**, 22, 4567-4574.

[14] Furukawa, T; Nakajima, T.; Takahashi, Y. Factors governing ferroelectric switching characteristics of thin VDF/TrFE copolymer films. *IEEE Dielectr Electr Insul* **2006**, 13, 1120-1131.

[15] Branciforti, M. C.; Sencadas, V.; Lanceros-Mendez, S.; Gregorio, R. Jr. New Technique of Processing Highly Oriented Poly(vinylidene fluoride) Films Exclusively in the β Phase. *J. Polym. Sci. Part B: Polym. Phys.* **2007**, 45, 2793-2801.

[16] Liu, Z. H.; Pan, C. T.; Yen, C. K.; Lin, L. W.; Huang, J. C.; Ke, C. A. Crystallization and mechanical behavior of the ferroelectric polymer nonwoven fiber fabrics for highly durable wearable sensor applications. *Appl. Surf. Sci*. **2015**, 291–301.

[17] Sencadas, V. Effect of the Processing Conditions on Morphology, Chain Orientation and Crystalline phases of PVDF and on Phase Transitions and Morphology of P(VDF-TrFE) Copolymers. Master Thesis, Universidade do Minho, Guimarães-Portugal, March 2005.

[18] Sencadas, V.; Moreira, V. M.; Lanceros-Mendéz, S.; Pouzada, A. S.; Gregorio, R. Jr. α-To-β transformation on PVDF films obtained by uniaxial stretch. *Mater. Sci. Forum* **2006**, 514-516, 872-876.

[19] Sajkiewicz, P.; Wasiak A.; Goclowski, Z. Phase transitions during stretching of poly(vinylidene-fuoride). *Eur. Polym. J.* **1999**, 35, 423-429.

[20] Siesler, H. W. Rheo-Optical Fourier-Transform Infrared Spectroscopy of Polyniers. 9. Stretching-induced II(α)-I(β) Crystal Phase Transformation in Poly(vinylidene fluoride). *J. Polym. Sci. Part B: Polym. Phys.* **1985**, 23, 2413-2422.

[21] Mhalgi, M. V.; Khakhar D. V.; Misra, A. Stretching Induced Phase Transformations in Melt Extruded Poly(vinylidene fluoride) Cast Films: Effect of Cast Roll Temperature and Speed. *Polym. Eng. Sci.* **2007**, 47, 1992-2004.

[22] Sencadas. V.; Gregorio, R. Jr.; Lanceros-Méndez, S. α to β Phase Transformation and Microstructural Changes of PVDF Films Induced by Uniaxial Stretch. *J. Macromol. Sci., Phys.* **2009**, 48, 514-525.

[23] Vijayakumar, R. P.; Khakhar, D. V.; Misra, A. Studies on α to β Phase Transformations in Mechanically Deformed PVDF Films. *J. Appl. Polym. Sci.* **2010**, 117, 3491–3497.

[24] Mohajir, B. E. E.; Heymans, N. Changes in structural and mechanical behaviour of PVDF with processing and thermomechanical treatments. 1. Change in structure. *Polymer* **2001**, 42, 5661-5667.

[25] Kepler R. G.; Anderson, R. A. Ferroelectricity in polyvinylidene fluoride. *J. Appl. Phys.* **1978**, 49, 1232.

[26] Mohammadi, B.; Yousefi, A. A.; Bellah, S. M. Effect of tensile strain rate and elongation on crystalline structure and piezoelectric properties of PVDF thin films. *Polym. Test.* **2007**, 26, 42-50.

[27] Maier, G. A.; Wallner, G.; Lang, R. W.; Fratzl, P. Structural changes during plastic deformation at crack tips in PVDF films: A scanning X-ray scattering study. *Macromolecules* **2005**, 38, 6099-6105.

[28] Matsushige, K.; Nagata, K.; Imada, S.; Takemura, T. The II-I crystal transformation of poly(vinylidene fluoride) under tensile and compressional stresses. *Polymer* **1980**, 21, 1391-1397.

[29] Carbeck, J. D.; Rutledge, G. C.; A Method for Studying Conformational Relaxations by Molecular Simulation: Conformational Defects in α-Phase Poly(vinylidene fluoride). *Macromolecules* **1996**, 29, 5190-5199.

[30] Takahashi, Y.; Miyaji, K. Long-Range Order Parameters of Form II of Poly(viny1idene fluoride) and Molecular Motion in the α_C Relaxation. *Macromolecules* **1983**, 16, 1789-1792.

[31] Li, L.; Zhang, M.; Rong M.; Ruan, W. Studies on the transformation process of PVDF from α to β phase by stretching. *RSC Adv.* **2014**, 4, 3938-3943.

[32] Guo, H.; Zhang, Y.; Xue, F.; Cai, Z.; Shang, Y.; Li, J.; Chen, Y.; Wu. Z.; Jiang, S. In situ synchrotron SAXS and WAXS investigations on deformation and α–β transformation of uniaxial stretched poly (vinylidene fluoride). *CrystEngComm* **2013**, 15, 1597-1606.

[33] Wu, J.; Schultz, J. M.; In situ simultaneous synchrotron small- and wide-angle X-ray scattering measurement of poly(vinylidene fluoride) fibers under deformation. *Macromolecules* **2000**, 33, 1765-1777.

[34] Zheng, H.; Wang, J.; Lofland, S. E.; Mohaddes-Ardabili, Z.; Ma.L.; Zhao, L. S. R. T.; Shinde, S. R.; Ogale, S. B.; Bai, F.; Viehland, D.; Jia, Y.; Schlom, D. G.; Wuttig, M.; Roytburd, A.; Ramesh, R. Multiferroic $BaTiO_3$-$CoFe_2O_4$ Nanostructures. *Science* **2004**, 303, 661-663.

[35] Mendes, S. F.; Costa, C. M.; Caparros, C.; Sencadas, V.; Lanceros-Mendez, S. Effect of filler size and concentration on the structure and properties of poly(vinylidene fluoride)/$BaTiO_3$ nanocomposites. *J. Mater. Sci.* **2012**, 47, 1378–1388.

[36] Jia, J.; Xing, Q.; Xia, G.; Sun, J.; Song. R.; Huang, W. Enhanced β-crystalline phase in poly(vinylidene fluoride) films by polydopamine-coated $BaTiO_3$ nanoparticles *Mater. Lett.* **2015**, 139, 212-215.

[37] Bodkhe, S.; Rajesh, P. S. M.; Kamle, S.; Verma, V. Beta-phase enhancement in polyvinylidene fluoride through filler addition: comparing cellulose with carbon nanotubes and clay. *J. Polym. Res.* **2014**, 21, 434.

[38] Sadeghi, F.; Ajji, A. Study of Crystal Structure of (Polyvinylidene fluoride/Clay) Nanocomposite Films: Effect of Process Conditions and Clay Type. *Polym. Eng. Sci.* **2009**, 49, 200-207.

[39] Umasankar, T. P.; Mhalgi, M. V.; Khakhar, D. V.; Misra, A. Studies on poly(vinylidene fluoride)–clay nanocomposites: Effect of different clay modifiers. *Polymer* **2008**, 49, 3486–3499.

[40] Martins, P.; Costa, C. M.; Ferreira, J. C. C.; Lanceros-Mendez, S. Correlation between Crystallization Kinetics and Electroactive Polymer Phase Nucleation in Ferrite/Poly(vinylidene fluoride) Magnetoelectric Nanocomposites. *J. Phys. Chem. B* **2012**, 794–801.

[41] Martins, P.; Costa C. M.; Lanceros-Mendez, S. Nucleation of electroactive β-phase poly(vinilidene fluoride) with $CoFe_2O_4$ and $NiFe_2O_4$ nanofillers: a new method for the preparation of multiferroic nanocomposites. *Appl. Phys. A* **2011**, 103, 233–237.

[42] Kelarakis, A.; Hayrapetyan, S.; Ansari, S.; Fang, J.; Estevez, L.; Giannelis, E. P. Clay nanocomposites based on poly(vinylidene fluoride-co-hexafluoropropylene): Structure and properties. *Polymer* **2010**, 51, 469–474.

[43] Dillon, D.R.; Tenneti, K. K.; Li, C. Y.; Ko, F. K; Sics, I.; Hsiao, B. S. On the strucure and morphology of polyvinylidene fluoride nanoclay-nanocomposites. *Polymer*, **2006**, 47, 1678–1688.

[44] Martins, P.; Lopes, A. C.; Lanceros-Mendez, S. Electroactive phases of poly(vinylidene fluoride): Determination, processing and applications. *Prog. Polym. Sci.* **2014**, 39, 683-706.

[45] Deka, S.; Joy, P. A.; Kumar, A. P. Single Step Synthesis and Properties of M/MFe_2O_4 and PVDF/M/MFe_2O_4 (M = Co, Ni) Magnetic Nanocomposites. *Sci. Adv. Mater.* **2009**, 1, 262-268.

[46] Ourry, L.; Marchesini, S.; Bibani, M.; Mercone, S.; Ammar S. ; Mammeri, F. Influence of nanoparticle size and concentration on the electroactive phase content of PVDF in PVDF–$CoFe_2O_4$-based hybrid films. *Phys. Status Solidi A* **2015**, 212, 252-258.

[47] Nunes, J. S.; Sencadas, V.; Wu, A.; Vilarinho, P. M.; Lanceros-Méndez, S. Electrical and Microstructural Changes of β-PVDF under Uniaxial Stress Studied by Scanning Force Microscopy. *Mater. Sci. Forum* **2006**, 514-516, 915-919.

[48] Liu, J.; Lu, X.; Wu, C. Effect of Preparation Methods on Crystallization Behavior and Tensile Strength of Poly(vinylidene fluoride). *Membranes* **2013**, 3, 389-405.

[49] Ribeiro, C.; Sencadas, V.; Ribelles, J. L. G.; Lanceros-Méndez, S. Influence of Processing Conditions on Polymorphism and Nanofiber Morphology of Electroactive Poly(vinylidene fluoride) Electrospun Membranes. *Soft. Mater.* **2010**, 8, 274-287.

[50] Lopes, A. C.; Costa, C. M.; Tavares, C. J.; Neves, I. C.; Lanceros-Mendez, S. Nucleation of the Electroactive γ Phase and Enhancement of the Optical Transparency in Low Filler Content Poly(vinylidene)/Clay Nanocomposites. *J. Chem. Phys. C* **2011**, 115, 18076-18082.

[51] Salimi, A.; Yousefi, A. A. FTIR studies of β-phase crystal formation in stretched PVDF films. *Polymer. Test.* **2003**, 22, 699-704.

[52] Esterly, D. M.; Love, B. J. Phase Transformation to β-Poly(vinylidene fluoride) by Milling. *J. Polym. Sci. Part B: Polym. Phys.* **2004**, 42, 91-97.

[53] G. T. Davis, Piezoelectric polymer transducers, *Institute for Materials Science and Engineering, National Bureau of Standards, Gaithersburg* 1987, 45-49.

[54] Ma, W.; Zhang, J.; Chen, S.; Wang, X. Crystalline phase formation of poly(vinylidene fluoride) from tetrahydrofuran/N,N-dimethylformamide mixed solutions. *J. Macromol. Sci., Phys.* **2008**, 47, 434-449.

[55] Liang, C. L.; Xie, Q.; Bao, R. Y.; Yang, W.; Xie, B. H. Yang, B. M. Induced formation of polar phases in poly(vinylidene fluoride) by cetyl trimethyl ammonium bromide. *J. Mater. Sci.* **2014**, 49, 4171-4179.

[56] Martins, P.; Costa. C. M.; Benelmekki. M.; Botelhob, G.; Lanceros-Mendez, S. On the origin of the electroactive poly(vinylidene fluoride) beta-phase nucleation by ferrite nanoparticles via surface electrostatic interactions. *CrystEngComm* **2012**, 14, 2807-2811.

[57] Sencadas, V.; Martins, P.; Pitaes, A.; Benelmekki, M.; Ribelles, J. L. G.; Lanceros-Mendez, S. Influence of Ferrite Nanoparticle Type and Content on the Crystallization Kinetics and Electroactive Phase Nucleation of Poly(vinylidene fluoride). *Langmuir* **2011**, 27, 7241–7249.

[58] Bhatt, A. S.; Bhat. D. K.; Santosh, M. S. Crystallinity, Conductivity, and Magnetic Properties of PVDF-Fe_3O_4 Composite Films. *J. Appl. Polym. Sci.* **2011**, 119, 968-972.

[59] Gaur, M. S.; Indolia, A. P.; Rogachev, A. A.; Rahachou, A. V. Influence of SiO_2 nanoparticles on morphological, thermal and dielectric properties of PVDF. *J. Therm. Anal. Calorim.* **2015**, 122, 1403-1416.

[60] Tiwari, V. K.; Prasad, A. K.; Singh, V.; Jana, K. K.; Misra, M.; Prasad C. D.; Maiti, P. Nanoparticle and Process Induced Super Toughened Piezoelectric Hybrid Materials: The Effect of Stretching on Filled System. *Macromolecules* **2013**, 46, 5595-5603.

[61] Kim, D.; Hong, S.; Hong, J.; Choi, Y.; Kim, J.; Park, M.; Sung T.; No, K. Fabrication of Vertically Aligned Ferroelectric Polyvinylidene Fluoride Mesoscale Rod Arrays. *J. Appl. Polym. Sci.* **2013**, 130, 3842–3848.

[62] Sun, L.L.; Li. B.; Zhang, Z. G.; Zhong, W. H. Achieving very high fraction of β-crystal PVDF and PVDF/CNF composites and their effect on AC conductivity and microstructure through a stretching process. *Eur. Polym. J.* **2010**, 46, 2112-2119.

[63] Thakur, P.; Kool, A.; Bagchi, B.; Das, S.; Papiya, N. Effect of in situ synthesized Fe_2O_3 and Co_3O_4 nanoparticles on electroactive β phase crystallization and dielectric properties of poly(vinylidene fluoride) thin films. *Phys. Chem. Chem. Phys.* **2015**, 17, 1368-1378.

Highlights

- Polymorphic α to β transformation induced by stretching is successfully monitored in flexible α-neat PVDF and α/β PVDF-$CoFe_2O_4$ based hybrid films, by coupling tensile test machine to near-field microscopy (AFM).
- $CoFe_2O_4$ NPs inclusions drastically change the crystallinity improvement mechanism observed in the β-phase transformation of hybrid self-standing films compared to the one of the α-neat PVDF films under stretching.
- The reinforcement of the elastic properties of the PVDF matrix by the NPs inclusions does not affect the deformation ability of the film.
- The stretching induced α to β transformation technique is promoted for the easy and low cost optimization processing of hybrid flexible films containing a small amount of magnetic inclusions.